

2014

Transient Exergy Destruction Analysis of a Vapor Compression System

Neera Jain

University of Illinois at Urbana-Champaign, United States of America, njain@alum.mit.edu

Andrew Alleyne

University of Illinois at Urbana-Champaign, United States of America, alleyne@illinois.edu

Follow this and additional works at: <http://docs.lib.purdue.edu/iracc>

Jain, Neera and Alleyne, Andrew, "Transient Exergy Destruction Analysis of a Vapor Compression System" (2014). *International Refrigeration and Air Conditioning Conference*. Paper 1542.
<http://docs.lib.purdue.edu/iracc/1542>

This document has been made available through Purdue e-Pubs, a service of the Purdue University Libraries. Please contact epubs@purdue.edu for additional information.

Complete proceedings may be acquired in print and on CD-ROM directly from the Ray W. Herrick Laboratories at <https://engineering.purdue.edu/Herrick/Events/orderlit.html>

Transient Exergy Destruction Analysis for a Vapor Compression System

Neera JAIN*, Andrew ALLEYNE

University of Illinois at Urbana-Champaign,
Urbana, IL, USA
njain@alum.mit.edu, alleyne@illinois.edu

* Corresponding Author

ABSTRACT

Through online optimization and control, vapor compression systems (VCSs) can effectively respond to disturbances, such as weather or varying loads that cannot be accounted for at the design stage, while simultaneously maximizing system efficiency. However, to do so requires a mathematical characterization of efficiency for the VCS. In particular, we would like to maximize the exergetic efficiency of the VCS which characterizes system efficiency relative to the maximum achievable efficiency as postulated by the second law of thermodynamics. This is equivalent to minimizing the rate of exergy destruction during system operation. Furthermore, in applications where VCSs encounter high frequency disturbances, such as in refrigerated transport applications or passenger vehicles, optimizing efficiency at steady-state conditions alone may not lead to significant reductions in energy consumption. Therefore, it is necessary to model the transient effects of changes in control variables on the rate of exergy destruction in a given system. In this paper we derive an expression for the transient rate of exergy destruction for the refrigerant-side dynamics of a VCS. A lumped parameter moving boundary modeling framework is used to model the two heat exchangers in the VCS. Open loop simulations using a validated nonlinear model of an experimental VCS are presented to highlight how changes in individual control variables affect the component-level and system-level exergy destruction rates as a function of time. The results are discussed in the context of their implication for exergy destruction-based optimal control.

1. INTRODUCTION

In order to meet the increasing demand for more efficient vapor compression systems (VCSs), effective control of these systems is required. Through online optimization and control, VCSs can effectively respond to disturbances such as changes in ambient conditions or time-varying thermal loads that cannot be accounted for at the design stage alone. Optimal control techniques can be used to simultaneously maximize both system performance and efficiency. However, to do so requires a mathematical characterization of these quantities. The most common efficiency metric used for VCSs is the coefficient of performance (COP), defined as the ratio of the heat energy removed to the energy consumed (by the VCS). This quantity is generally greater than one. However, the maximum achievable COP is limited by the temperatures of the hot and cold environments that interact with the VCS (Stoecker & Jones, 1983). Therefore, it is more informative to consider the second law, or exergetic, efficiency, η_{II} , which characterizes efficiency relative to the maximum achievable efficiency as postulated by the second law of thermodynamics.

$$0 \leq \eta_{II} = \left\{ 1 - \frac{\text{exergy destroyed}}{\text{exergy supplied}} \right\} < 1 \quad (1)$$

Exergy analyses have been used extensively in the thermodynamics community to understand the source of irreversibilities in a variety of thermal systems, thereby influencing design changes at the system or component level (Kotas, 1985). In the context of VCSs, Ahamed, Saidur, and Masjuki (2011) provide an extensive review of exergy analyses that have been conducted, particularly highlighting the effect of different refrigerants, as well as key parameters such as evaporating temperature, on the exergetic efficiency of the system. More recently, Mahabadipour and Ghaebi (2012) used an exergy analysis to evaluate the better of two designs of expander cycles for refrigeration systems. In addition to exergy analyses, researchers have used exergy destruction minimization (EDM), also known as entropy generation minimization or thermodynamic optimization (Bejan, 2002), to optimize

design and operational parameters in many thermal systems from a static point of view. For example, design parameters such as heat exchanger geometry have been optimized using EDM (Nag & De, 1997) (Vargas & Bejan, 2001). As can be seen from Eq. (1), minimizing the exergy destroyed in a system will maximize the exergetic efficiency.

In applications where VCSs encounter high frequency disturbances, such as in refrigerated transport trucks and trailers or passenger vehicles, optimizing efficiency at steady-state conditions alone may not lead to significant reductions in energy consumption. Therefore, the goal of this paper is to enable the use of EDM in conjunction with optimal control techniques by modeling the *transient* effects of changes in control variables on the rate of exergy destruction in a given system. In this paper we derive an expression for the transient rate of exergy destruction for the refrigerant-side dynamics of a vapor-compression system (VCS) using a lumped parameter moving boundary modeling framework for the heat exchangers. To the knowledge of the authors, this is the first characterization of the transient exergy destruction rate in a VCS.

The paper is organized as follows. Preliminaries, including an introduction to exergy, are provided in Section 2. The derivation of the transient exergy destruction rate in a VCS is described in Section 3. Simulation results using a validated nonlinear VCS model are presented in Section 4 that show how changes in individual control variables affect the component-level and system-level exergy destruction rates. The results are discussed in the context of their implication for exergy destruction-based optimal control.

2. PRELIMINARIES

2.1 Exergy

Exergy (also referred to as “availability”) is defined as the maximum reversible work that can be extracted from a substance at a given state during its interaction with a given environment (Çengel and Boles, 2008). Whereas energy is always conserved, exergy is not. Similarly to energy, exergy can be transferred in three ways: by heat transfer, work, or through mass exchange with the environment. However, contrary to energy, exergy is destroyed during irreversible phenomena such as chemical reactions, mixing, and viscous dissipation. The rate of change of exergy in a control volume is defined mathematically as

$$\frac{dX_{cv}}{dt} = \frac{dE_{cv}}{dt} - T_0 \frac{dS_{cv}}{dt} = \sum_j \left(1 - \frac{T_0}{T_j} \right) \dot{Q}_j - \left(\dot{W}_{cv} - P_0 \frac{dV_{cv}}{dt} \right) + \sum_i \dot{m}_i \psi_i - \sum_o \dot{m}_o \psi_o - \dot{X}_{dest} \quad (2)$$

where \dot{Q}_j is the heat transfer rate at the location on the control volume boundary where the instantaneous temperature is T_j . The specific flow exergy, ψ , is defined as

$$\psi = (h - h_0) - T_0 (s - s_0) + \frac{v^2}{2} + gz + \psi^{ch} \quad (3)$$

where the quantities T_0 , P_0 , h_0 , and s_0 are the temperature, pressure, specific enthalpy, and specific entropy, respectively, of the reference environment. The reference environment is typically chosen as an infinite reservoir with which the system is interacting, such as the ambient environment. The amount of exergy destroyed in a system or through a process is a measure of the loss of potential to do work and is proportional to the amount of entropy generated in the system as shown in Eq. (4).

$$\dot{X}_{dest} = T_0 \dot{S}_{gen} \quad (4)$$

2.2 VCS Modeling

For dynamic modeling of the heat exchangers, two different approaches have been primarily used: a finite-volume approach and a lumped parameter moving boundary approach (Rasmussen B. P., 2012). In the lumped parameter moving boundary modeling approach, the heat exchanger is modeled with a fixed number of fluid regions (defined by fluid phase), and the location of the boundary between each fluid region is a dynamic variable, allowing the length of the fluid regions to vary. Fluid properties such as temperature, density, etc., are lumped in each region, and an average is used for model computations. Although this approach results in some loss in accuracy as

compared to finite-volume approaches, the resulting models are of low dynamic order, making them well suited for control design. A review of the literature shows that this approach has been applied to a variety of VCSs, often with variations in the details of the modeling approach (Bendapudi & Braun, May 2002). The condenser and evaporator models that are used as the basis for the derivation of the transient exergy destruction rate in this paper are described in detail in McKinley and Alleyne (2008) and Li and Alleyne (2010).

3. DERIVATION OF TRANSIENT EXERGY DESTRUCTION RATE

To develop a dynamic expression for the total rate of exergy destruction in a standard VCS, it is necessary to consider each component individually as a control volume, as shown in Figure 1. The total rate of exergy destruction in a four-component VCS is a sum of the rates of exergy destruction in each individual component:

$$\dot{X}_{dest,VCC} = \dot{X}_{dest,k} + \dot{X}_{dest,v} + \dot{X}_{dest,c} + \dot{X}_{dest,e}. \quad (5)$$

Note that the evaporator and condenser fans are not considered in this analysis for the purpose of illustrative clarity. They could be added if needed, but the refrigerant-focused construct here is sufficient for characterizing the transient exergy destruction rate in the VCS.

In the following sections, the exergy destruction rate for each component in a standard VCS will be derived. The reference temperature, T_0 , for the exergy calculation is assumed to be the temperature of the high-temperature reservoir (i.e. ambient environment), T_H .

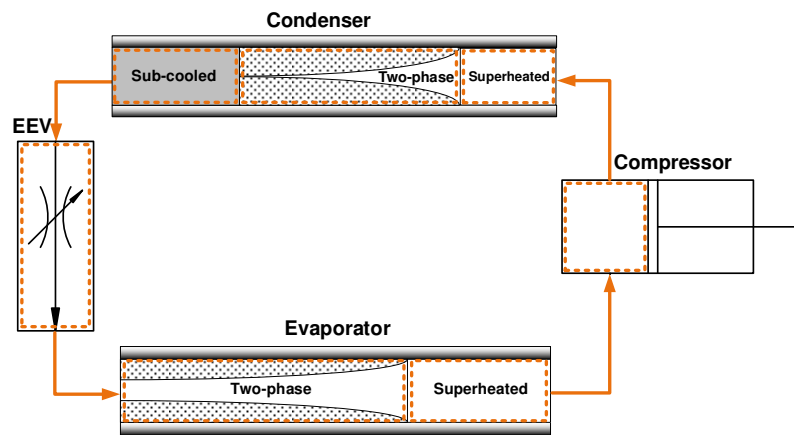


Figure 1: Schematic depicting control volumes drawn inside each component of the VCS.

3.1 Compressor and EEV

In VCS modeling, both the compressor and expansion device, assumed here to be an electronic expansion valve (EEV), are typically modeled using quasi-steady assumptions. Therefore, the compressor and EEV control volumes can be analyzed assuming that they are operating at steady-state. The compressor is assumed to be adiabatic but not isentropic. Therefore, there is no exergy transfer by heat. A control volume is defined around the refrigerant inside the compressor as shown in Figure 1. The inlet and outlet mass flow rates are equal to the refrigerant mass flow rate through the compressor. Assuming steady state operation, Eq. (2) reduces to

$$-(-\dot{W}_k) + \dot{m}_{r,k} (\psi_{k,i} - \psi_{k,o}) - \dot{X}_{dest,k} = 0. \quad (6)$$

The effects of kinetic and potential energy are assumed to be negligible. Substituting Eq. (3) into Eq. (7) and simplifying yields

$$\dot{X}_{dest,k} = -(-\dot{W}_k) + \dot{m}_{r,k} \left[(h_{k,ri} - h_{k,ro}) - T_H (s_{k,ri} - s_{k,ro}) \right]. \quad (7)$$

Note that the work transfer rate term in Eq. (7) must be a positive quantity because if the compressor was isentropic, then the rate of exergy destruction would equal zero (and $h_{k,ri} - h_{k,ro}$ is a negative quantity). Therefore, we write $-(-\dot{W}_k)$ to emphasize the fact that the sign convention for work done *on* the system is negative, where

$$\dot{W}_k = \dot{m}_{r,k} (h_{k,ro} - h_{k,ri}). \quad (8)$$

The rate of exergy destruction in the compressor is determined by substituting Eq. (8) into Eq. (7) and simplifying:

$$\dot{X}_{dest,k} = -T_H \dot{m}_{r,k} (s_{k,ri} - s_{k,ro}). \quad (9)$$

To derive the rate of exergy destruction in the EEV, a control volume is defined around the refrigerant in the EEV. The expansion of the refrigerant is assumed to be isenthalpic (i.e. $h_{v,ri} = h_{v,ro}$). There is only exergy transfer by mass transfer, and the inlet and outlet mass flow rates are equal to the refrigerant mass flow rate through the EEV. Assuming steady-state operation and regarding the effects of kinetic and potential energy as negligible gives

$$\dot{X}_{dest,v} = -T_H \dot{m}_{r,v} (s_{v,ri} - s_{v,ro}). \quad (10)$$

3.2 Heat Exchangers

The remaining components are the two heat exchangers: the evaporator and the condenser. The dynamics of these components dominate the overall dynamics of the cycle; consequently, transient rates of exergy destruction through each of these components will be derived.

In the lumped parameter moving boundary modeling approach, the evaporator is typically modeled with two fluid regions: a two-phase refrigerant fluid region and a superheated refrigerant fluid region. In this way, separate lumped parameters are used to estimate the fluid properties in each of the fluid regions, thereby improving the accuracy of the estimates. Similarly, two separate control volumes are used to derive the total exergy destruction rate through the evaporator as shown in Figure 2.

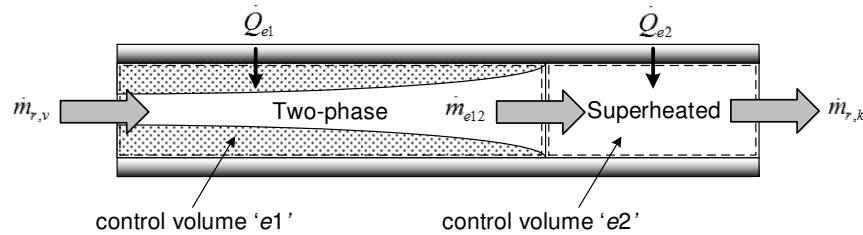


Figure 2: Individual control volumes drawn around each fluid region in an evaporator.

For the two-phase refrigerant fluid region, denoted by the subscript $e1$, Eq. (2) reduces to

$$\frac{dX_{e1}}{dt} = \left(1 - \frac{T_H}{T_{w,e1}}\right) \dot{Q}_{e1} + P_0 \frac{dV_{e1}}{dt} + \dot{m}_{r,v} (h_{e,ri} - T_H s_{e,ri}) - \dot{m}_{e12} (h_{e,g} - T_H s_{e,g}) - \dot{X}_{dest,e1}, \quad (11)$$

where T_j is replaced with $T_{w,e1}$, the lumped tube wall temperature in the two-phase fluid region, and \dot{m}_{e12} is the refrigerant mass flow rate between the two control volumes pictured in Figure 2. Similarly, for the superheated refrigerant fluid region, denoted by the subscript $e2$, Eq. (2) reduces to

$$\frac{dX_{e2}}{dt} = \left(1 - \frac{T_H}{T_{w,e2}}\right) \dot{Q}_{e2} + P_0 \frac{dV_{e2}}{dt} + \dot{m}_{e12} (h_{e,g} - T_H s_g) - \dot{m}_{r,k} (h_{e,ro} - T_H s_{e,ro}) - \dot{X}_{dest,e2}, \quad (12)$$

where T_j is replaced with $T_{w,e2}$, the lumped tube wall temperature in the superheated fluid region. Applying superposition allows us to express $\dot{X}_{dest,e}$ as

$$\dot{X}_{dest,e} = \dot{X}_{dest,e1} + \dot{X}_{dest,e2}. \quad (13)$$

Therefore, the total exergy destruction rate through the evaporator is

$$\begin{aligned} \dot{X}_{dest,e} = & \left(1 - \frac{T_H}{T_{w,e1}}\right) \dot{Q}_{e1} + \left(1 - \frac{T_H}{T_{w,e2}}\right) \dot{Q}_{e2} + P_0 \left(\frac{dV_{e1}}{dt} + \frac{dV_{e2}}{dt}\right) + \dot{m}_{r,v} (h_{e,ri} - T_H s_{e,ri}) \\ & - \dot{m}_{r,k} (h_{e,ro} - T_H s_{e,ro}) - \left(\frac{dX_{e1}}{dt} + \frac{dX_{e2}}{dt}\right). \end{aligned} \quad (14)$$

where it is assumed that

$$\dot{Q}_e = \dot{Q}_{e1} + \dot{Q}_{e2} = (UA)_{e1} (T_{w,e1} - T_{r,e1}) + (UA)_{e2} (T_{w,e2} - T_{r,e2}). \quad (15)$$

In other words, it is assumed that there is no heat transfer between the refrigerant in control volume $e1$ and the refrigerant in control volume $e2$. In Eq. (15), $T_{r,e1}$ and $T_{r,e2}$ refer to the lumped refrigerant temperature in each fluid region, and $(UA)_{e1}$ and $(UA)_{e2}$ are the overall heat transfer coefficients between the refrigerant and tube wall in each fluid region.

An alternative method for deriving the exergy destruction rate is to perform an entropy balance on the control volume using Eq. (16), solve for the rate of entropy generation \dot{S}_{gen} , and then scale \dot{S}_{gen} by the reference environment temperature, T_0 , as shown in Eq. (4).

$$\frac{dS_{cv}}{dt} = \sum_j \frac{\dot{Q}_j}{T_j} + \sum_i \dot{m}_i s_i - \sum_o \dot{m}_o s_o + \dot{S}_{gen} \quad (16)$$

Because it is difficult to evaluate dX_{cv}/dt , the entropy rate balance given in Eq. (16) can be used to derive an expression for the exergy destruction rate in terms of dS_{cv}/dt instead of dX_{cv}/dt . Applying Eq. (16) to each control volume of the evaporator yields

$$\frac{dS_{e1}}{dt} = \frac{\dot{Q}_{e1}}{T_{w,e1}} + (\dot{m}_{r,v} s_{e,ri} - \dot{m}_{e12} s_{e,g}) + \dot{S}_{gen,e1}, \quad (17)$$

$$\frac{dS_{e2}}{dt} = \frac{\dot{Q}_{e2}}{T_{w,e2}} + (\dot{m}_{e12} s_{e,g} - \dot{m}_{r,k} s_{e,ro}) + \dot{S}_{gen,e2}, \quad (18)$$

where

$$\dot{S}_{gen,e} = \dot{S}_{gen,e1} + \dot{S}_{gen,e2}. \quad (19)$$

Substituting Eq. (17) and Eq. (18) into Eq. (19) and rearranging yields the following alternative expression for the exergy destruction rate in the evaporator:

$$\dot{X}_{dest,e} = T_H \dot{S}_{gen,e} = -T_H \left(\frac{\dot{Q}_{e1}}{T_{w,e1}} + \frac{\dot{Q}_{e2}}{T_{w,e2}} \right) - (\dot{m}_{r,v} T_H s_{e,ri} - \dot{m}_{r,k} T_H s_{e,ro}) + T_H \left(\frac{dS_{e1}}{dt} + \frac{dS_{e2}}{dt} \right). \quad (20)$$

Expressions for dS_{e1}/dt and dS_{e2}/dt will be derived in Section 3.3.

In the lumped parameter moving boundary modeling approach, the condenser is typically modeled with three refrigerant fluid regions: a superheated fluid region, a two-phase fluid region, and a subcooled fluid region. To remain consistent with the modeling approach, three separate control volumes are used to derive the total exergy destruction rate through the condenser as shown in Figure 3. Although at steady-state it can be assumed that the heat transfer out of the condenser is occurring at the reference temperature, T_H , the control volumes defined in Figure 3 for the condenser only contain the refrigerant flowing through the condenser tube. Therefore, the transfer of heat away from the refrigerant is occurring at the tube wall temperatures of each fluid region. The procedure for deriving the total exergy destruction rate through the condenser is analogous to the procedure described for the evaporator, and so we present only the final result in Eq. (21),

$$\begin{aligned} \dot{X}_{dest,c} = & \left(1 - \frac{T_H}{T_{w,c1}}\right)(-\dot{Q}_{c1}) + \left(1 - \frac{T_H}{T_{w,c2}}\right)(-\dot{Q}_{c2}) + \left(1 - \frac{T_H}{T_{w,c3}}\right)(-\dot{Q}_{c3}) + P_0 \left(\frac{dV_{c1}}{dt} + \frac{dV_{c2}}{dt} + \frac{dV_{c3}}{dt}\right) \\ & + \dot{m}_{r,k} (h_{c,ri} - T_H s_{c,ri}) - \dot{m}_{r,v} (h_{c,ro} - T_H s_{c,ro}) - \left(\frac{dX_{c1}}{dt} + \frac{dX_{c2}}{dt} + \frac{dX_{c3}}{dt}\right) \end{aligned} \quad (21)$$

which is equivalent to

$$\dot{X}_{dest,c} = T_H \dot{S}_{gen,c} = T_H \left(\frac{\dot{Q}_{c1}}{T_{w,c1}} + \frac{\dot{Q}_{c2}}{T_{w,c2}} + \frac{\dot{Q}_{c3}}{T_{w,c3}}\right) - (\dot{m}_{r,k} T_H s_{c,ri} - \dot{m}_{r,v} T_H s_{c,ro}) + T_H \left(\frac{dS_{c1}}{dt} + \frac{dS_{c2}}{dt} + \frac{dS_{c3}}{dt}\right). \quad (22)$$

We assume that there is no heat transfer between the refrigerant in control volumes $c1$, $c2$, and $c3$ so that $\dot{Q}_c = \dot{Q}_{c1} + \dot{Q}_{c2} + \dot{Q}_{c3}$. Expressions for dS_{ci}/dt , $i=\{1,2,3\}$, will be derived in the next section.

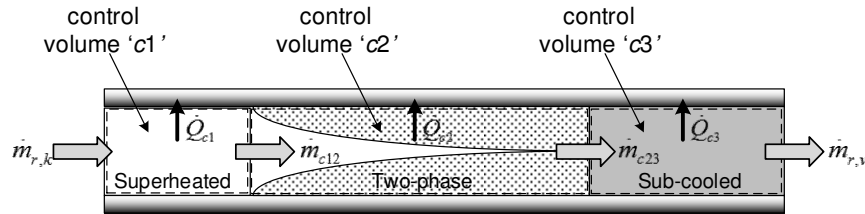


Figure 3: Individual control volumes drawn around each fluid region in a condenser.

3.3 The Entropy Differential

The rate of change of entropy is described as

$$\frac{dS_{cv}}{dt} = s_{cv} \frac{dm_{cv}}{dt} + m_{cv} \left(\left. \frac{(\partial s_{cv})}{\partial h} \right|_P \frac{dh}{dt} + \left. \frac{(\partial s_{cv})}{\partial P} \right|_h \frac{dP}{dt} \right). \quad (23)$$

In Eq. (23) the dependent variables are chosen as specific enthalpy and pressure, but they can be chosen as any two independent thermodynamic state variables. Equation (23) also highlights why it is helpful to define multiple control volumes for the heat exchangers in which a separate control volume is drawn around each fluid region (recall Figure 2). This formulation allows for lumped parameters to be used to approximate s_{cv} and m_{cv} for each control volume as is done in the lumped parameter moving boundary modeling approach. The expression for dm_{cv}/dt can be derived in the lumped parameter moving boundary framework for each control volume as described in Rasmussen (2000).

For the two-phase fluid region of the evaporator, refrigerant mean void fraction, rather than specific enthalpy, and pressure will be used to describe specific entropy, as shown in Eq. (24),

$$\frac{dS_{e1}}{dt} = s_{e1} \frac{dm_{e1}}{dt} + m_{e1} \left(\left. \frac{(\partial s_{e1})}{\partial \bar{\gamma}_e} \right|_P \frac{d\bar{\gamma}_e}{dt} + \left. \frac{(\partial s_{e1})}{\partial P_e} \right|_{\bar{\gamma}} \frac{dP_e}{dt} \right) \quad (24)$$

where $m_{e1} = \rho_{e1} \zeta_{e1} L_{R,e} A_{CR,e}$,

$$\frac{dm_{e1}}{dt} = (\dot{m}_{r,v} - \dot{m}_{e12}) + \rho_{e1} A_{CR,e} L_{R,e} \frac{d\zeta_{e1}}{dt}, \quad (25)$$

and

$$s_{e1} = \bar{x}_e s_{e,g} + (1 - \bar{x}_e) s_{e,l} = \frac{\bar{\gamma}_e \rho_{e,g} s_{e,g} + (1 - \bar{\gamma}_e) \rho_{e,l} s_{e,l}}{\bar{\gamma}_e \rho_{e,g} + (1 - \bar{\gamma}_e) \rho_{e,l}}. \quad (26)$$

Mean void fraction, $\bar{\gamma}$, is related to mean quality, \bar{x} , by the following relationship:

$$\bar{x} = \bar{\gamma} \frac{\rho_g}{\rho} \quad (27)$$

Moreover, the variables $\rho_{e,l}$, $\rho_{e,g}$, $s_{e,l}$ and $s_{e,g}$ are all solely functions of pressure. The partial derivatives $\left. \frac{\partial s_{e,l}}{\partial \bar{\gamma}_e} \right|_p$ and $\left. \frac{\partial s_{e,l}}{\partial P_e} \right|_{\bar{\gamma}}$, shown in Eq. (28) and Eq. (29) respectively, are derived using Eq. (26).

$$\left. \frac{\partial s_{e,l}}{\partial \bar{\gamma}_e} \right|_p = \frac{(\bar{\gamma}_e \rho_{e,g} + (1 - \bar{\gamma}_e) \rho_{e,l})(\rho_{e,g} s_{e,g} - \rho_{e,l} s_{e,l}) - (\bar{\gamma}_e \rho_{e,g} s_{e,g} + (1 - \bar{\gamma}_e) \rho_{e,l} s_{e,l})(\rho_{e,g} - \rho_{e,l})}{(\bar{\gamma}_e \rho_{e,g} + (1 - \bar{\gamma}_e) \rho_{e,l})^2} \quad (28)$$

$$\begin{aligned} \left. \frac{\partial s_{e,l}}{\partial P_e} \right|_{\bar{\gamma}} &= \frac{\beta_1 - \beta_2}{\beta_3} \\ \beta_1 &= (\bar{\gamma}_e \rho_{e,g} + (1 - \bar{\gamma}_e) \rho_{e,l}) \left(\bar{\gamma}_e \rho_{e,g} \frac{ds_{e,g}}{dP_e} + s_{e,g} \bar{\gamma}_e \frac{d\rho_{e,g}}{dP_e} + (1 - \bar{\gamma}_e) \rho_{e,l} \frac{ds_{e,l}}{dP_e} + s_{e,l} (1 - \bar{\gamma}_e) \frac{d\rho_{e,l}}{dP_e} \right) \\ \beta_2 &= (\bar{\gamma}_e \rho_{e,g} s_{e,g} + (1 - \bar{\gamma}_e) \rho_{e,l} s_{e,l}) \left(\bar{\gamma}_e \frac{d\rho_{e,g}}{dP_e} + (1 - \bar{\gamma}_e) \frac{d\rho_{e,l}}{dP_e} \right) \\ \beta_3 &= (\bar{\gamma}_e \rho_{e,g} + (1 - \bar{\gamma}_e) \rho_{e,l})^2 \end{aligned} \quad (29)$$

Evaluating Eq. (23) for the superheated fluid region of the evaporator yields

$$\frac{ds_{e2}}{dt} = s_{e2} \frac{dm_{e2}}{dt} + \rho_{e2} \zeta_{e2} L_{R,e} A_{CR,e} \left(\left. \frac{\partial s_{e2}}{\partial h_{e2}} \right|_p \frac{dh_{e2}}{dt} + \left. \frac{\partial s_{e2}}{\partial P_e} \right|_h \frac{dP_e}{dt} \right) \quad (30)$$

where

$$\frac{dm_{e2}}{dt} = (\dot{m}_{e12} - \dot{m}_{r,k}) + \rho_{g,e} A_{CR,e} L_{R,e} \frac{d\zeta_{e1}}{dt} \quad (31)$$

A procedure analogous to the one described above can be used to determine the rate of change of entropy in each of the condenser control volumes: ds_{ci}/dt , $i=\{1,2,3\}$. It is assumed that the outlet refrigerant condition of the condenser is subcooled liquid; therefore, the condenser is characterized using three fluid regions. As in the case of the evaporator, specific enthalpy and pressure are used to describe specific entropy in the superheated and subcooled fluid regions, and mean void fraction and pressure are used in the two-phase fluid region. The expressions for ds_{ci}/dt , $i = \{1,2,3\}$ are given in Eqs. (32) – (37), respectively.

$$\frac{ds_{c1}}{dt} = s_{c1} \frac{dm_{c1}}{dt} + \rho_{c1} \zeta_{c1} L_{R,c} A_{CR,c} \left(\left. \frac{\partial s_{c1}}{\partial h_{c1}} \right|_p \frac{dh_{c1}}{dt} + \left. \frac{\partial s_{c1}}{\partial P_c} \right|_h \frac{dP_c}{dt} \right) \quad (32)$$

$$\frac{dm_{c1}}{dt} = (\dot{m}_{r,k} - \dot{m}_{c12}) + \rho_{g,c} A_{CR,c} L_{R,c} \frac{d\zeta_{c1}}{dt} \quad (33)$$

$$\frac{ds_{e2}}{dt} = s_{c2} \frac{dm_{c2}}{dt} + \rho_{c2} \zeta_{c2} L_{R,c} A_{CR,c} \left(\left. \frac{\partial s_{c2}}{\partial \bar{\gamma}_c} \right|_p \frac{d\bar{\gamma}_c}{dt} + \left. \frac{\partial s_{c2}}{\partial P_c} \right|_{\bar{\gamma}} \frac{dP_c}{dt} \right) \quad (34)$$

$$\frac{dm_{c2}}{dt} = (\dot{m}_{c12} - \dot{m}_{c23}) + \rho_{l,c} A_{CR,c} L_{R,c} \left(\frac{d\zeta_{c1}}{dt} + \frac{d\zeta_{c2}}{dt} \right) - \rho_{g,c} A_{CR,c} L_{R,c} \frac{d\zeta_{c1}}{dt} \quad (35)$$

$$\frac{dS_{c3}}{dt} = s_{c3} \frac{dm_{c3}}{dt} + \rho_{c3} \zeta_{c3} L_{R,c} A_{CR,c} \left(\left. \frac{(\partial S_{c3})}{\partial h_{c3}} \right|_p \frac{dh_{c3}}{dt} + \left. \frac{(\partial S_{c3})}{\partial P_c} \right|_h \frac{dP_c}{dt} \right) \quad (36)$$

$$\frac{dm_{c3}}{dt} = (\dot{m}_{c23} - \dot{m}_{r,v}) - \rho_{l,c} A_{CR,c} L_{R,c} \left(\frac{d\zeta_{c1}}{dt} + \frac{d\zeta_{c2}}{dt} \right) \quad (37)$$

Substituting Eqs. (9), (10), (20), and (22) into Eq. (5) and simplifying results in

$$\dot{X}_{dest,VCS} = T_H \left(\frac{\dot{Q}_{c1}}{T_{w,c1}} + \frac{\dot{Q}_{c2}}{T_{w,c2}} + \frac{\dot{Q}_{c3}}{T_{w,c3}} - \frac{\dot{Q}_{e1}}{T_{w,e1}} - \frac{\dot{Q}_{e2}}{T_{w,e2}} \right) + T_H \left(\frac{dS_{e1}}{dt} + \frac{dS_{e2}}{dt} + \frac{dS_{c1}}{dt} + \frac{dS_{c2}}{dt} + \frac{dS_{c3}}{dt} \right), \quad (38)$$

the instantaneous exergy destruction rate in the VCS.

4. SIMULATION

To explore the effect of changes in control inputs on the transient exergy destruction rate in a VCS, a 1kW VCS was modeled and simulated using the Air Force Research Laboratory (AFRL) Transient Thermal Modeling and Optimization (ATTMO) toolbox (Kania, et al., 2012) which is based on the THERMOSYS Toolbox (Alleyne, 2012) from the University of Illinois at Urbana-Champaign. To demonstrate importance of characterizing the transient exergy destruction in the VCS, the compressor speed was increased by 300 rpm in two cases. In Case 1, the rate limit of the compressor was set to 15 rpm/second, and in Case 2, the rate limit of the compressor was set to 1 rpm/second.

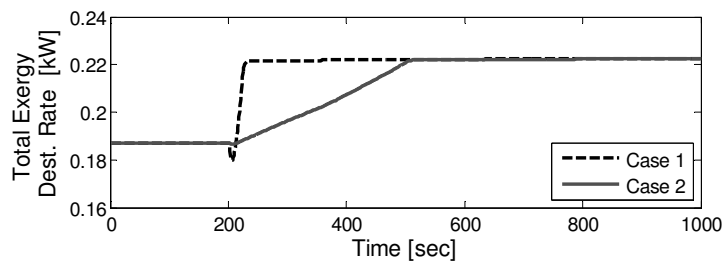


Figure 4: Total exergy destruction rate resulting from increase in compressor speed by 300 rpm at $t=200$ seconds for two different rate limits.

As shown in Figure 4, by slowly ramping the compressor speed in Case 2, the total exergy destruction rate is lower during the transient than in Case 1. Figure 5 shows how the rate of exergy destruction in each individual component changes as a function of the change in the compressor speed for both Case 1 and Case 2. It is clear from Figure 4 and Figure 5 how the operation of the compressor during a transient (such as a decrease in the room temperature setpoint) affects the exergy destruction rate in the system and thereby its exergetic efficiency. Certainly, increasing the rate at which the compressor speed increases will decrease the time to pull down the room temperature; however, this comes at a cost that we can quantify from an exergetic perspective. Using the model for total transient exergy destruction rate derived in this paper, we can explore ways to balance these competing objectives from an operational perspective. It is also worth noting that the exergy destruction rates in the evaporator and condenser actually decrease briefly during the transient in Case 1. In future work we will explore tradeoffs between reductions in the exergy destruction rate of one component versus another, particularly when all four control inputs are changing simultaneously.

Similar results to those presented here for an increase in the compressor speed can be reproduced for the other control inputs in the VCS: EEV aperture, evaporator fan speed, and condenser fan speed. We are interested in designing feedback controllers that make coordinated decisions about how to operate the different actuators in the

system so that at any given time, the VCS is balancing its multiple control objectives, e.g. maximizing exergetic efficiency while minimizing room temperature pull down time.

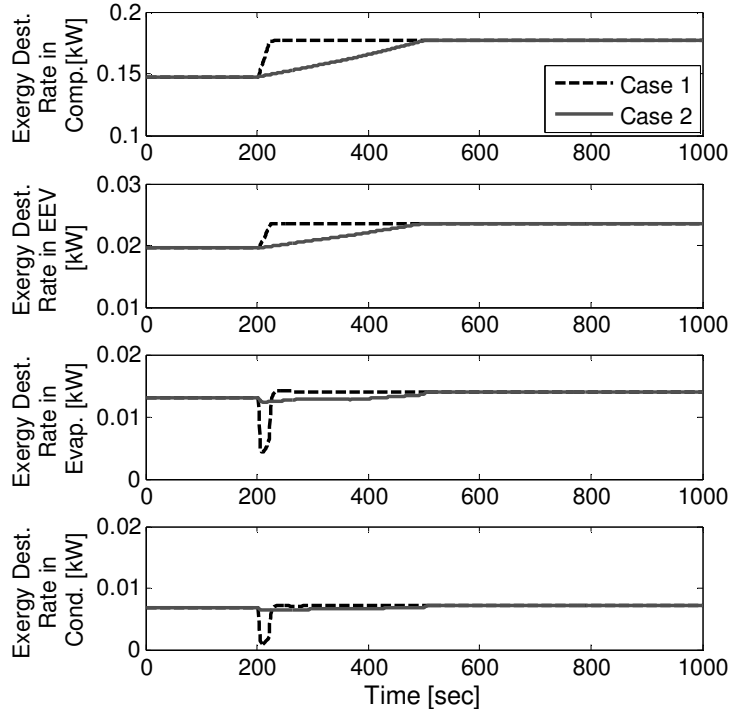


Figure 5: Rate of exergy destruction by component resulting from increase in compressor speed by 300 rpm at $t=200$ seconds for two different rate limits.

5. CONCLUSION

Through online optimization and control, vapor compression systems (VCSs) can effectively respond to disturbances, such as weather or varying loads that cannot be accounted for at the design stage, while simultaneously maximizing system efficiency. In this paper we derived an expression for the transient rate of exergy destruction for the refrigerant-side dynamics of a VCS that enables the use of exergy destruction minimization (EDM) in conjunction with optimal control techniques for efficient operation of a VCS. A lumped parameter moving boundary modeling framework was used to characterize the two heat exchangers in the VCS, and lumped fluid regions were used to define multiple control volumes within each heat exchanger. Open loop simulations of a nonlinear VCS model showed how the exergy destruction rate in individual components, and the overall system, is affected dynamically by changes in the control inputs, such as compressor speed. Future work will include the study of EDM during real-time operation of VCSs through the design of optimal controllers that minimize exergy-based objective functions. Additionally, the analysis of the heat exchangers will be extended to include irreversibilities arising from the interaction between the heat exchanger and the secondary side fluid.

NOMENCLATURE

A	area	m^2	Subscript
a	aperture	% of maximum	a air
E	energy	kJ	c condenser
h	specific enthalpy	$\text{kJ}\cdot\text{kg}^{-1}$	$c1$ superheated fluid region in condenser
L	length	m	$c2$ two-phase fluid region in condenser
m	mass	kg	$c3$ subcooled fluid region in condenser
\dot{m}	mass flow rate	$\text{kg}\cdot\text{s}^{-1}$	CR cross-sectional area
P	pressure	kPa	cv control volume

\dot{Q}	heat transfer rate	kW	<i>dest</i>	destroyed
S	entropy	$\text{kJ}\cdot\text{K}^{-1}$	<i>e</i>	evaporator
s	specific entropy	$\text{kJ}\cdot(\text{kg}\cdot\text{K})^{-1}$	<i>e1</i>	two-phase fluid region in evaporator
T	temperature	K	<i>e2</i>	superheated fluid region in evaporator
t	time	s	<i>g</i>	gaseous state
UA	overall heat transfer coefficient	$\text{kJ}\cdot(\text{s}\cdot\text{K})^{-1}$	<i>gen</i>	generation
V	volume	m^3	<i>H</i>	high temperature environment
v	velocity	$\text{m}\cdot\text{s}^{-1}$	<i>i</i>	in (inlet)
\dot{W}	work transfer rate (power)	kW	<i>k</i>	compressor
X	exergy	kJ	<i>L</i>	low temperature environment
\dot{X}	exergy transfer rate	kW	<i>l</i>	liquid state
\bar{x}	mean quality	dimensionless	<i>o</i>	outlet
\bar{v}	mean void fraction	dimensionless	<i>r,R</i>	refrigerant
ζ	normalized zone length	dimensionless	<i>v</i>	EEV
η	efficiency	dimensionless	<i>w</i>	wall
ρ	density	$\text{kg}\cdot\text{m}^{-3}$	0	reference environment
ψ	specific flow exergy	$\text{kJ}\cdot\text{kg}^{-1}$	12	between the first and second fluid regions
			23	between the second and third fluid regions

REFERENCES

- Ahamed, J. U., Saidur, R., & Masjuki, H. H. (2011). A review on exergy analysis of vapor compression refrigeration system. *Renewable and Sustainable Energy Reviews*, 15(3), 1593-1600.
- Alleyne, A. (2012). THERMOSYS 4 Toolbox. University of Illinois at Urbana-Champaign. Retrieved from <http://arg.mechse.illinois.edu/thermosys/>
- Bejan, A. (2002). Fundamentals of exergy analysis, entropy generation minimization, and the generation of flow architecture. *International Journal of Energy Research*, 26, 545-565.
- Bendapudi, S., & Braun, J. E. (May 2002). *A Review of Literature on Dynamic Models of Vapor Compression Equipment*. ASHRAE Report #4036-5.
- Cengel, Y. A., & Boles, M. A. (2008). *Thermodynamics: An Engineering Approach* (6th ed.). Boston: The McGraw-Hill Companies, Inc.
- Kania, M., Koeln, J., Alleyne, A., McCarthy, K., Wu, N., & Patnaik, S. (2012). A Dynamic Modeling Toolbox for Air Vehicle Vapor Cycle Systems. *SAE Power Systems International*. Phoenix, AZ.
- Kotas, T. J. (1985). *The Exergy Method of Thermal Plant Analysis*. London: Butterworths.
- Li, B., & Alleyne, A. G. (2010). A dynamic model of a vapor compression cycle with shut-down and start-up operations. *International Journal of Refrigeration*, 33(3), 538-552.
- Mahabadipour, H., & Ghaebi, H. (2012). Development and comparison of two expander cycles used in refrigeration system of olefin plant based on exergy analysis. *Applied Thermal Engineering*, 50(1), 771-780.
- McKinley, T. L., & Alleyne, A. G. (2008). An advanced nonlinear switched heat exchanger model for vapor compression cycles using the moving-boundary method. *International Journal of Refrigeration*, 31(7), 1253-1264.
- Nag, P. K., & De, S. (1997). Design and Operation of a Heat Recovery Steam Generator with Minimum Irreversibility. *Applied Thermal Engineering*, 17(4), 385-391.
- Rasmussen, B. (2005). *Dynamic Modeling and Advanced Control of Air Conditioning and Refrigeration Systems*. Urbana, IL: Ph.D. Dissertation, Dept. Mech. Eng., Univ. Illinois Urbana-Champaign.
- Rasmussen, B. P. (2000). Control-Oriented Modeling of Transcritical Vapor Compression Systems. Urbana, IL: University of Illinois at Urbana-Champaign, M.S. Thesis.
- Rasmussen, B. P. (2012). Dynamic modeling for vapor compression systems - Part I: Literature Review. *HVAC&R Research*, 18(5), 934-955.
- Stoecker, W., & Jones, J. (1983). *Refrigeration and Air-Conditioning*. New York: McGraw-Hill Book Company.
- Vargas, J., & Bejan, A. (2001). Thermodynamic optimization of finned crossflow heat exchangers for aircraft environmental control systems. *International Journal of Heat and Fluid Flow*, 22, 657-665.